Exp Brain Res (1995) 106:79–92

RESEARCH ARTICLE

Scott Manaker · Patrick F. Fogarty

Raphespinal and reticulospinal neurons project to the dorsal vagal complex in the rat

Received: 9 August 1994 / Accepted: 6 March 1995

Abstract Stimulation of the caudal raphe nuclei alters visceral functions. The caudal raphe nuclei project to the nucleus of the solitary tract, which receives the central terminations of vagal afferents and plays an important role in the central integration of autonomic activities. The caudal raphe nuclei also project to the somatic and preganglionic autonomic motoneurons of the spinal cord. Diamidino yellow was injected into the nucleus of the solitary tract, and fast blue was injected into either the cervical, thoracic, or lumbar spinal cord. Large numbers of double-labeled neurons were present within the caudal raphe nuclei and the adjacent reticular formation of the medial tegmental field. This observation documents that individual raphespinal and reticulospinal neurons project an axon collateral to the nucleus of the solitary tract. These data demonstrate the anatomic substrate for global modulation of the autonomic motoneuron pool by the caudal raphe nuclei.

Key words Autonomic · Axon collaterals · Medial tegmental field · Motoneurons · Respiratory · Rat

Introduction

The nucleus of the solitary tract (NST) plays an important role in the integration of autonomic nervous system function (Spyer 1982; Sawchenko 1983). The caudal NST receives the primary terminations of vagal visceral afferents (Contreras et al. 1982; Kalia and Sullivan 1982; Leslie et al. 1982; Shapiro and Miselis 1985; Altschuler et al. 1989, 1991). Reciprocal connectivity exists between the NST and other regions participating in the central nervous integration of autonomic function, including the paraventricular hypothalamic nucleus (Saper et al. 1976; Ricardo and Koh 1978; Sawchenko and Swanson 1982; Van der Kooy et al. 1984; ter Horst et al. 1989; Lynn et al. 1991), the rostroventrolateral nucleus (Ross et al. 1985), and the parabrachial nucleus (Norgren 1978; Ricardo and Koh 1978; Saper and Loewy 1980; Herbert et al. 1990). The NST projects to the vagal preganglionic motoneurons in both the dorsal motor nucleus of the vagus and the nucleus ambiguus (Norgren 1978; Ricardo and Koh 1978; Ross et al. 1985) and also projects to the sympathetic preganglionic motoneurons in the intermediolateral column of the spinal cord (Loewy and Burton 1978; Holstege et al. 1979; Loewy 1981; Loewy and McKellar 1981; Morrison and Gebber 1984, 1985; Bacon and Smith 1990), allowing direct modulation of autonomic outflow pathways.

Similar to its role in the autonomic nervous system, the NST also has a central role in the neural control of respiration (Feldman 1986). Carotid body (Finley and Katz 1992) and pulmonary (Kalia and Sullivan 1982; Bonham and McCrimmon 1990; Bonham and Joad 1991) vagal afferents terminate in the NST. The NST contains the physiologically defined respiratory neurons of the dorsal respiratory group (Saether et al. 1987; Ezure et al. 1988) and reciprocally projects to the ventral medullary (Yamada et al. 1988; Connelly et al. 1989; Smith et al. 1989; Ellenberger and Feldman 1990) and pontine (Smith et al. 1989) groups of respiratory neurons.

The caudal raphe nuclei, including the nuclei raphe magnus, obscurus, and pallidus are important sources of central afferents to the NST. These raphe neurons, as well as neurons in the adjacent reticular formation of the medial tegmental field, directly project to the NST (Basbaum et al. 1978; Rogers et al. 1980; Ross et al. 1981; Thor and Helke 1987, 1989; Schaffar et al. 1988; Lynn et al. 1991). Furthermore, a variety of experimental studies

S. Manaker · P.F. Fogarty
Department of Medicine (Pulmonary and Critical Care Division) and Pharmacology, Center for Sleep and Respiratory Neurobiology, and Institute of Neurological Sciences, University of Pennsylvania School of Medicine, Philadelphia, Pa., USA

S. Manaker (✉)
987 Maloney Building, Pulmonary and Critical Care Division, Hospital of the University of Pennsylvania, 3600 Spruce Street, Philadelphia, PA 19104-4283, USA;
Fax: +1-215-349-5172

have demonstrated stimulation of the caudal raphe nuclei alters autonomic activity (Polc and Monnier 1970; Adair et al. 1977; McCann et al. 1989; Hornby et al. 1990; Carruth et al. 1992) and respiration (Sessle et al. 1981; Holtman et al. 1986a, b, 1987; Lalley 1986a, b; Millhorn 1986; Morin et al. 1990). However, the physiologic significance of these effects of raphe stimulation has not yet been completely elucidated.

Caudal raphe and adjacent reticular formation neurons have highly collateralized axons, which may be quite divergent. Axons from individual raphespinal and reticulospinal neurons collateralize to both cervical and lumbar spinal cord (Hayes and Rustioni 1981; Huisman et al. 1981, 1982; Martin et al. 1981a; Lovick and Robinson 1983). In addition, raphespinal axon collaterals have been demonstrated to the sensory trigeminal nucleus (Lovick and Robinson 1983; Li et al. 1993), periaqueductal gray (Kwiat and Basbaum 1990), medial preoptic area (Leanza et al. 1991), and hypoglossal nucleus (Manaker et al. 1992).

We hypothesized that the projection from the caudal raphe nuclei to the NST (Basbaum et al. 1978; Rogers et al. 1980; Ross et al. 1981; Thor and Helke 1987, 1989; Schaffar et al. 1988; Lynn et al. 1991) might represent an axon collateral from raphespinal neurons also projecting to autonomic or respiratory regions of the spinal cord. Therefore, the double retrograde fluorescent tracer technique developed by Kuypers and colleagues (Kuypers and Huisman 1984) was employed. Injection of diamidino yellow (DY) into the NST, combined with injection of fast blue (FB) into either the cervical, thoracic, or lumbar spinal cord produced large numbers of double-labeled neurons in the caudal raphe nuclei and adjacent reticular formation of the medial tegmental field. These results demonstrate that individual neurons of the caudal raphe nuclei and adjacent regions of the ventromedial reticular formation collateralize to both the NST and the spinal cord. This observation documents the existence of an anatomic substrate for widespread modulation of the autonomic nervous system by the caudal raphe nuclei (Holstege 1991; Jacobs and Azmitia 1992).

Materials and methods

Animals

Male Sprague-Dawley rats (200–400 g; Charles River, Wilmington, Mass.) were maintained on a 14-h/10-h light/dark cycle, with food and water ad libitum, and fasted overnight prior to fluorescent tracer injection. Postoperatively, all rats were able to spontaneously ambulate, ingest food and water, and groom.

Surgery and tracer injections

All rats received injections of two tracers. To search for neurons projecting to both the spinal cord and the NST, all animals were injected with DY (3% in distilled water) into the NST and with FB (3% in distilled water) into either the fifth cervical (n=3), fourth thoracic (n=3), or second lumbar (n=3) spinal segment.

Rats were anesthetized with pentobarbital (75 mg/kg intraperitoneally), and tracer injections were performed on the left side. Tracer injections were performed with glass micropipettes (100 μm diameter) secured on a 10-μl Hamilton microsyringe, and large tracer volumes (2–4 μl) were employed to maximize the detection of double-labeled neurons. For spinal cord injections, a laminectomy was performed at either C_5, T_4, or L_2. Tracer injections were centered in the ventral gray matter of cervical and lumbar spinal cord; while the thoracic spinal cord injections were centered in the lateral region of the intermediate zone, adjacent to the autonomic motoneuron pool. A micropipette was lowered into the gray matter of cervical and thoracic cord according to the following coordinates: 0.6 mm lateral to the midline and 1.4 mm deep from the dorsal surface of the spinal cord. For lumbar cord, the coordinates were similar, except that the micropipette was advanced 1.5 mm deep. For NST injections, the caudal portion of the occipital bone was removed and a micropipette was introduced according to the following coordinates: 0.1 mm rostral to the caudal border of the area postrema, 0.7 mm lateral to the midline, and 0.5 mm deep perpendicular to the dorsal medullary surface.

A 4-μl volume of tracer was attempted for each injection. The tracer injection was halted if tracer appeared at the surface of the brain or spinal cord from around the micropipette shaft. Any excess tracer was rinsed away with saline. For over half of the tracer injections, the full 4 μl volume was successfully injected (Table 1) without spillage.

Three series of rats served as controls for the large-volume injections utilized. The first series served to document the presence of double-labeled neurons without use of large tracer volumes. In three animals, 200 nl DY was injected into NST and 50 nl FB was injected into the cervical spinal cord, while in another rat 50 nl DY was injected into the NST and 4 μl FB was injected into the cervical spinal cord. A series of animals served to control for the spread of DY into the fourth ventricle. Five rats were injected with 4 μl FB into the cervical spinal cord, and 1–3 μl DY was injected into the fourth ventricle.

Table 1 Number of diamidino yellow- (DY) and fast blue- (FB)-labeled neurons in the medial tegmental field. DY and FB were each injected into either the NST or the spinal cord, as described in the text. The injection volume for each tracer and site, the survival time, and the number of neurons retrogradely labeled by DY alone, FB alone, or both (double-labeled) are listed. The numbers reflect neuron counts from every ninth section from each animal

Case	Diamidino yellow		Fast blue		Survival time (days)	Number of labeled neurons		
	Injection site	Injection volume (μl)	Injection site	Injection volume (μl)		DY	FB	FB+DY
1	NST	4.0	Cervical	4.0	16	751	2106	672
2	NST	4.0	Cervical	4.0	10	463	1593	470
3	NST	4.0	Cervical	4.0	12	1255	2220	769
4	NST	3.6	Thoracic	3.6	23	933	1203	576
5	NST	2.0	Thoracic	2.0	20	1035	1357	880
6	NST	4.0	Thoracic	4.0	19	1070	1740	952
7	NST	4.0	Lumbar	4.0	32	1834	628	1103
8	NST	3.2	Lumbar	3.0	31	1057	1063	798
9	NST	3.3	Lumbar	3.6	32	976	1163	359

The final series of animals controlled for the spread of DY into structures adjacent to the NST. Injections of DY centered in the gracile nucleus were performed according to the following coordinates: 0.4 mm caudal to the caudal border of the area postrema, 0.4 mm lateral to the midline, and 0.1 mm deep perpendicular to the dorsal medullary surface. One rat had 1 µl FB injected into the cervical spinal cord and 1 µl DY injected into the gracile nucleus. Three additional rats had 4 µl FB injected into the cervical spinal cord and either 1 µl, 1.5 µl, or 2 µl DY injected into the gracile nucleus. No more than 2 µl of DY could be injected into the gracile nucleus without efflux of tracer to the brainstem surface from around the micropipette shaft.

Fig. 1A–D Fluorescent labeling in caudal raphe nuclei with fast blue (FB) and diamidino yellow (DY). **A** FB cytoplasmic fluorescence in nucleus raphe obscurus. Note the absence of nuclear labeling. **B** A single double-labeled neuron with both DY nuclear and FB cytoplasmic fluorescence in nucleus raphe magnus. **C** DY nuclear fluorescence and double-labeled neuron with both DY nuclear and FB cytoplasmic fluorescence in nucleus raphe magnus. **D** A single neuron labeled with DY nuclear fluorescence and a single neuron labeled with FB cytoplasmic fluorescence in nucleus raphe magnus. The two brightly labeled neurons in the *upper left* are double-labeled neurons out of the focal plane. *Thick, filled arrows*, neuron displaying only nuclear fluorescence from DY; *thick, empty arrow*, neuron displaying only cytoplasmic fluorescence from FB; *thin arrow*, double-labeled neuron displaying both nuclear fluorescence from DY and cytoplasmic fluorescence from FB. *Scale bar* 10 µm for **A–C**; 15 µm for **D**

Histology

On the basis of preliminary studies and our previous results (Manaker et al. 1992), rats were allowed to survive for periods of up to 32 days (Table 1) to allow maximal retrograde transport and neuronal labeling. After the survival period, rats were anesthetized with pentobarbital (150 mg/kg intraperitoneally) and transcardially perfused with 100 ml clearing solution (6% dextran, heparin 3000 U/l; 20 °C), followed by 500 ml fixative (10% paraformaldehyde, 50 mM phosphate buffer; 20 °C) and then 500 ml cryoprotectant (10% sucrose, 100 mM phosphate buffer; 10 °C). The brain and spinal cord were then dissected out, and placed overnight in a

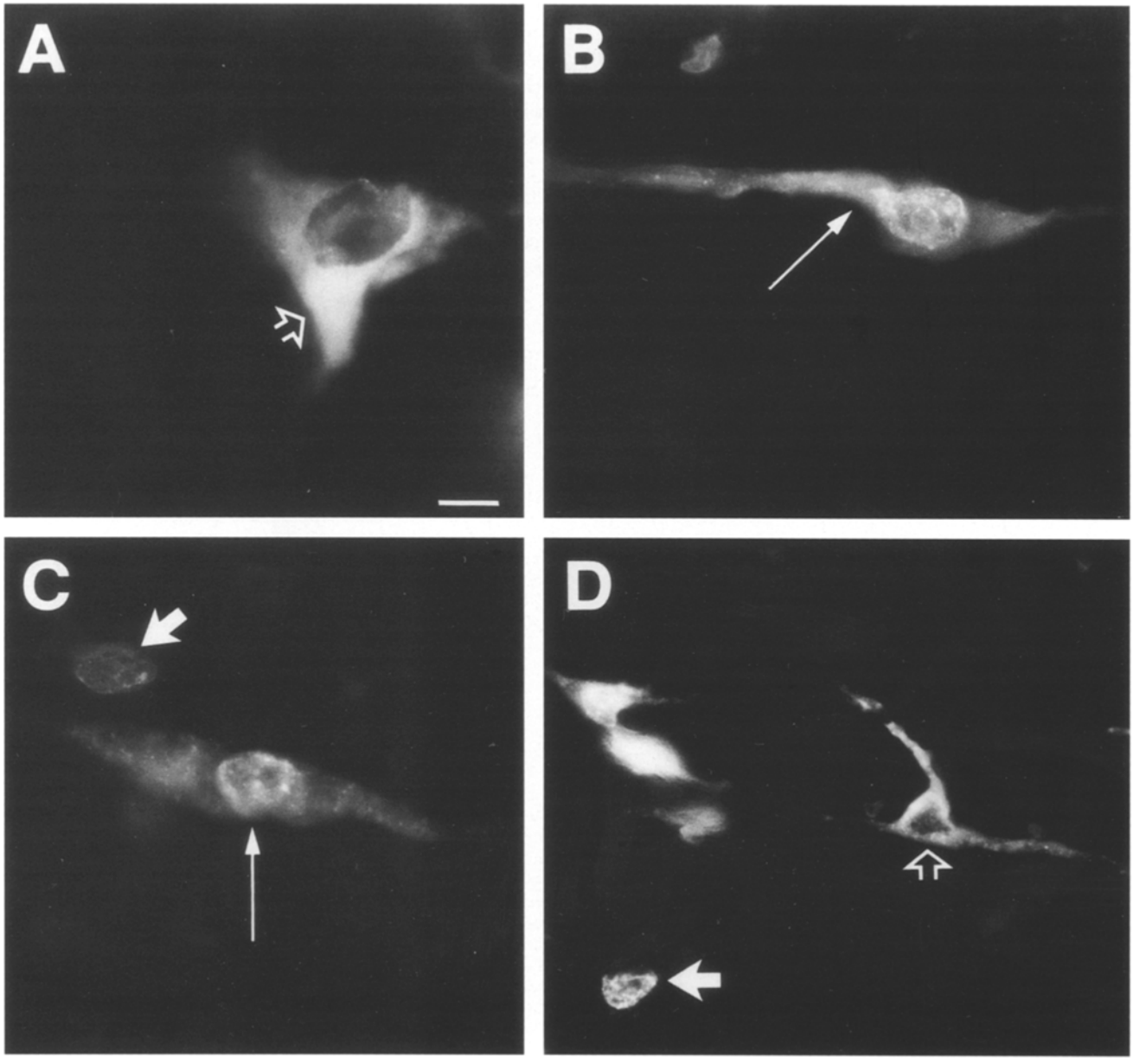

second cryoprotectant (30% sucrose, 100 mM phosphate buffer; pH 7.3; 10 °C). Tissues were then blocked, mounted on cryostat chucks, and frozen in dry ice. Sequential sections 32 μm thick were cut at −18 °C, thaw-mounted on gelatin/chromate-coated slides, coverslipped with DPX Mountant (Electron Microscopy Sciences, Fort Washington, Pa), and stored with desiccant at −17° C until examination.

Microscopy, photography, and data analysis

Sections through the medulla and pons were examined under epifluorescence with a Leitz Aristoplan microscope. FB fluorescent neurons were defined as only those somata with cytoplasm filled with blue-white fluorescence, a dark nonfluorescing nucleus, and at least one clearly discernible neuronal process (Fig. 1). DY fluorescent neurons were defined as containing the characteristic granular yellow nucleus (Fig. 1). Neurons double-labeled, containing both FB and DY, were identified by their filled cytoplasm and brigthly fluorescing nuclei (Fig. 1). No leakage of DY or FB from neuronal somata was observed with the survival times utilized in the present study. Fluorescent neurons were counted from every ninth section and manually plotted on camera lucida line drawings derived from adjacent sections stained with cresyl violet. The atlas and nomenclature of Paxinos and Watson (1986) was utilized, and neurons were placed within anatomic boundaries as defined by regional cytoarchitecture (e.g., Andrezik and Beitz 1985; Newman 1985a, b). The analysis was limited to the caudal raphe nuclei and adjacent reticular formation nuclei of the medial tegmental field (as originally defined by Holstege and Kuypers 1977), where neurons with divergent axon collaterals have previously been demonstrated (Hayes and Rustioni 1981; Huisman et al. 1981, 1982; Martin et al. 1981a; Lovick and Robinson 1983; Kwiat and Basbaum 1990; Leanza et al. 1991; Manaker et al. 1992). Photography was performed with a Kodak T-Max 400. Data are presented as means±standard errors.

Results

Injection site analysis

Tracer spread into adjacent structures from the injection site centers was unavoidable with the relatively large volume of tracers employed in these studies (Fig. 2). Therefore, we now describe the injection sites of the nine cases included in our quantitative analysis and our control injection sites in the fourth ventricle and the gracile nucleus.

Nucleus of the solitary tract. Injections of DY centered in the NST (n=9) produced tracer extending into the adjacent dorsal motor nucleus of the vagus, the area postrema, and the gracile nucleus. In no case did unabsorbed

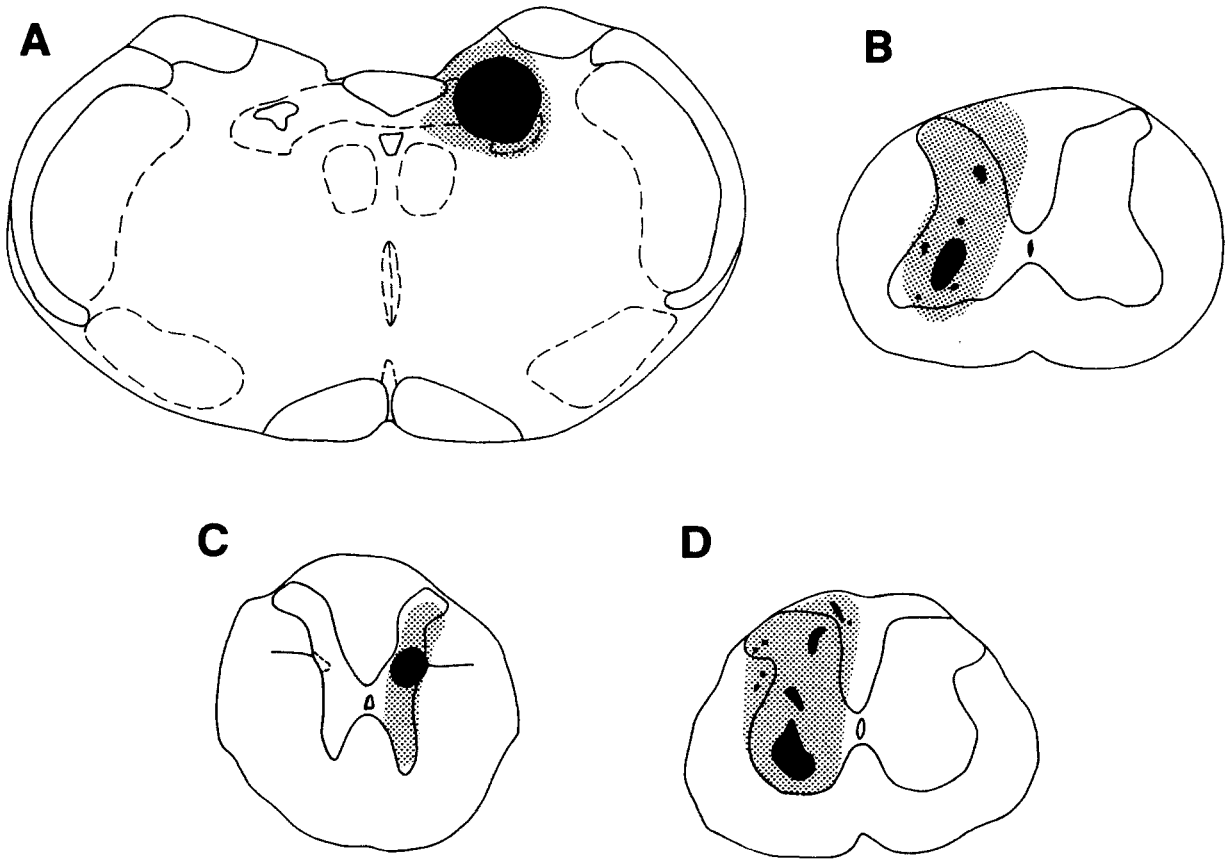

Fig. 2A–D Line drawings depicting representative tracer injection sites. *Black*, central necrosis and residual tracer; *gray shading*, many glia and neurons, all intensely labeled with tracer. **A** Example of a section through the center of an injection site after diamidino yellow (DY) was injected into the nucleus of the solitary tract. **B** Example through the center of an injection site after fast blue (FB) was injected into the fifth cervical segment. **C** Example through the center of an injection site after FB was injected into the third thoracic segment. **D** Example through the center of an injection site after FB was injected into the second lumbar segment

tracer or the central zone of necrosis extend into the hypoglossal nucleus. Similarly, cases with local spread of DY from the NST into the adjacent reticular formation were excluded from these studies. The tracer within the NST was limited to the intermediate and caudal regions of the nucleus and did not extend into the rostral regions of the nucleus.

Cervical spinal cord. Injections of FB (n=3) into the fifth cervical segment were all centered and most extensive in the ventral gray matter, although necrosis and unabsorbed tracer were also observed in the dorsal gray matter. The injection site extended rostrally and caudally for up to one spinal segment in each direction. The medial and lateral motoneuronal columns were heavily infiltrated with tracer, including the caudal portions of the phrenic nucleus. Necrotic material and residual tracer were also noted up to, but not crossing, the contralateral rim of the central canal. There was moderate extension of the injection site into adjacent regions of the dorsal and lateral funiculi, and minimal extension of the injection site into the ventral and ventrolateral tracts.

Thoracic spinal cord. Injections of FB (n=3) into the fourth thoracic segment produced injection sites centered in the intermediomedial and intermediolateral cell columns, although the entire gray matter was heavily infiltrated with tracer. As in cervical spinal cord, the injection site extended rostrally and caudally for one spinal segment each. Residual tracer and necrosis were spread throughout the gray matter ipsilaterally and extended into the dorsal and lateral funiculi, but minimally into the ventral and ventrolateral funiculi.

Lumbar spinal cord. Injections of FB (n=3) into the second lumbar segment produced similar results as in cervical spinal cord. The injection site extended rostrally and caudally for one spinal segment each. The entire ventral gray was heavily infiltrated with tracer. Necrosis and residual tracer were centered in the ventral gray but spread throughout the ipsilateral gray matter. The injection site extended only moderately into the dorsal and lateral funiculi and minimally into the ventral and ventrolateral funiculi.

Gracile nucleus. Injection of DY into the gracile nucleus produced an injection site centered in the gracile nucleus, with some spread into the superficial regions of the area postrema, but with no tracer evident in the NST in three of the four cases. In one case, after injection of 1.5 µl DY into the gracile nucleus, a small amount of tracer spread into the adjacent NST.

Fourth ventricle. Injections of DY into the fourth ventricle produced nuclear labeling all along the dorsal surface of the medulla, and particularly within the area postrema. Often, a large quantity of injected tracer could be identified within the fourth ventricle.

Number of labeled neurons

Larger numbers of medial tegmental field neurons retrogradely labeled by DY injections into the NST (Table 1) were observed in association with lumbar injections of FB into the spinal cord than with cervical or thoracic injections. In cases with cervical injections of FB, the fewest neurons (1434±318) were retrogradely labeled by DY injected into the NST. More DY-labeled neurons (1815±156) were observed in those cases receiving FB injections into the thoracic cord, and the highest numbers of retrogradely labeled DY neurons (2042±472) were noted in cases following FB injections into the lumbar cord.

In contrast, the largest numbers of FB labeled neurons were observed after FB was injected into the cervical region (2610±280 neurons). The numbers of neurons in the medial tegmental field retrogradely labeled with FB were intermediate after thoracic FB injections (2236±264 neurons) and smallest after tracer injection into the lumbal spinal cord (1705±99 neurons).

Distribution of labeled neurons

Large numbers of neurons retrogradely labeled with DY, FB, or both fluorescent tracers were observed within all the nuclei and subregions of the medial tegmental field (Table 2, Fig. 3). The largest numbers of neurons retrogradely labeled by DY injected into the NST were observed bilaterally within the lateral paragigantocellular nucleus, with moderate numbers of neurons present throughout the adjacent reticular formation and caudal raphe nuclei of the medial tegmental field. This labeling pattern is consistent with previous studies of the afferent connectivity of the NST (Basbaum et al. 1978; Rogers et al. 1980; Ross et al. 1981; Thor and Helke 1987, 1989; Schaffar et al. 1988; Lynn et al. 1991).

Large numbers of neurons in the pars alpha and pars ventralis of the gigantocellular reticular nucleus were retrogradely labeled by FB injected into the spinal cord at either the cervical, thoracic, or lumbar levels. Many neurons with cytoplasmic FB fluorescence in the caudal raphe nuclei, and a moderate number of FB-labeled somata located within the paramedian, lateral paragigantocellular, and ventral pontine reticular nuclei projected to each level of the spinal cord. The distribution of retrograde FB labeling is in close accord with previous descriptions of the brainstem afferents to the spinal cord (for review, see Holstege 1991). Therefore, only the localization of neurons double-labeled by both DY injected into the NST and FB injected into the spinal cord will be described in detail.

The highest densities of double-labeled neurons were observed in the nuclei raphe pallidus and obscurus (Fig. 3). Quantitatively, the highest percentages of double-labeled neurons were noted within the caudal raphe nuclei, while the highest absolute numbers of double-labeled neurons were contained within the gigantocellular reticular nucleus, pars alpha.

Table 2 Distribution of diamidino yellow- (*DY*) and fast blue- (*FB*) -labeled neurons in the medial tegmental field. Number of labeled neurons within the caudal raphe nuclei and adjacent regions of the ventromedial reticular formation after injections of DY and FB. The number of neurons retrogradely labeled by DY alone, FB alone, or both (double-labeled) is listed. The numbers reflect neuron counts from every ninth section from each animal. (*NST* nucleus of solitary tract)

Injection site Tracer injected		NST DY	Cervical FB	*N*=3 DY+FB	NST DY	Thoracic FB	*N*=3 DY+FB	NST DY	Lumbar FB	*N*=3 DY+FB
Medial tegmental field nuclei										
Raphe pallidus	(mean±SEM)	33±6	137±13	45±4	32±10	115±15	73±20	61±10	35±6	41±13
	(range)	26–45	114–159	38–50	12–47	89–142	32–94	42–76	26–47	15–57
Raphe obscurus	(mean±SEM)	57±35	198±52	77±20	60±14	105±21	69±21	99±31	49±9	62±25
	(range)	21–128	146–302	56–117	33–79	76–145	41–111	47–149	38–67	11–89
Raphe magnus										
Ipsilateral	(mean±SEM)	32±18	155±17	78±9	43±11	108±14	85±8	60±6	90±19	68±15
	(range)	13–68	124–184	65–94	23–62	93–136	73–100	48–69	55–121	50–97
Contralateral	(mean±SEM)	36±4	127±9	56±6	52±4	80±19	59±16	66±9	56±17	52±13
	(range)	28–42	110–140	48–69	44–59	43–108	30–83	56–84	28–88	28–72
Gigantocellular, pars alpha										
Ipsilateral	(mean±SEM)	73±10	284±49	100±26	143±44	208±30	153±11	85±23	186±45	103±28
	(range)	56–90	230–389	70–153	84–229	150–252	132–168	51–128	104–259	64–157
Contralateral	(mean±SEM)	88±17	200±22	67±7	117±33	162±37	94±9	93±13	129±24	71±14
	(range)	67–122	157–228	54–78	76–182	104–230	80–111	79–119	102–177	45–95
Gigantocellular, pars ventralis										
Ipsilateral	(mean±SEM)	54±32	206±65	57±23	50±9	198±22	64±13	85±29	139±41	71±26
	(range)	17–118	76–275	17–94	33–63	155–230	41–85	49–143	81–217	32–121
Contralateral	(mean±SEM)	57±33	204±56	40±21	57±13	146±40	55±12	81±18	87± 21	79±40
	(range)	15–121	100–294	16–81	35–80	88–222	34–76	47–105	46–117	27–158
Lateral paragigantocellular										
Ipsilateral	(mean±SEM)	134±38	72±12	23±7	153±26	43±18	40±17	228±51	45±17	63±31
	(range)	71–203	48–89	12–35	102–184	15–77	6–60	168–330	13–70	21–123
Contralateral	(mean±SEM)	129±41	61±11	16±7	150±24	38±10	29±6	217±47	15±5	38±17
	(range)	67–206	41–77	9–29	102–180	18–51	19–41	157–309	6–22	9–67
Paramedian reticular										
Ipsilateral	(mean±SEM)	34±7	105±6	26±3	46±7	112±8	30±8	76±40	50±9	26±17
	(range)	27–47	93–113	23–32	33–57	101–128	15–43	20–153	33–64	9–59
Contralateral	(mean±SEM)	47±8	103±5	21±1	63±24	90±22	26±10	85±22	27±8	36±23
	(range)	35–61	97–112	20–22	20–102	53–128	6–39	53–128	14–40	12–82
Ventral pontine reticular										
Ipsilateral	(mean±SEM)	22±12	50±3	17±5	20±3	14±1	16±6	30±10	23±8	26±15
	(range)	6–45	47–77	12–33	17–26	13–16	6–25	13–48	20–33	10–56
Contralateral	(mean±SEM)	26±9	36±10	13±1	27±5	13±5	9±4	22±8	11±1	17±14
	(range)	9–37	20–55	8–15	19–37	4–21	2–15	14–38	10–13	2–45

Caudal raphe nuclei

Within each of the caudal raphe nuclei (nuclei raphe pallidus, obscurus, and magnus), a high percentage of the neuronal afferents to the NST originated from raphespinal neurons (Table 2, Fig. 3). Almost 70% of the neurons in the nucleus raphe pallidus that were retrogradely labeled by DY injected into the NST also projected an axon collateral to the thoracic spinal cord. Over 50% of all the neurons in the nuclei raphe obscurus and magnus that were retrogradely labeled by NST DY injections likewise projected to the thoracic spinal cord. Similarly, within the nuclei raphe pallidus and obscurus and bilaterally within the nucleus raphe magnus, over 50% of the raphe neurons projecting to the NST also projected to the cervical spinal cord. Large numbers of caudal raphe neurons were also double-labeled by DY injected into the NST and FB injected into the lumbar spinal cord. The percentage of caudal raphe neurons projecting to the NST that simultaneously innervated the lumbar spinal cord ranged from 39% in the nucleus raphe pallidus to 53% in the nucleus raphe magnus ipsilateral to the DY injection site.

When quantified as those raphespinal neurons projecting to the NST, lower percentages of double-labeled neurons were observed for all the caudal raphe nuclei at all levels of the spinal cord. The highest percentages of double-labeled neurons were present in the nuclei raphe obscurus and pallidus, where about 55% of the neurons projecting to the lumbar spinal cord also projected an axon collateral to the NST. A moderate percentage (39–48%) of afferents from the nucleus raphe magnus to the lumbar spinal cord and from all the caudal raphe nuclei to the thoracic spinal cord were double-labeled from DY injected into the NST. Lower percentages (<30%) of raphespinal afferents to the cervical spinal cord were double-labeled by DY injected into the NST, particularly within the nucleus raphe magnus ipsilateral to the DY in-

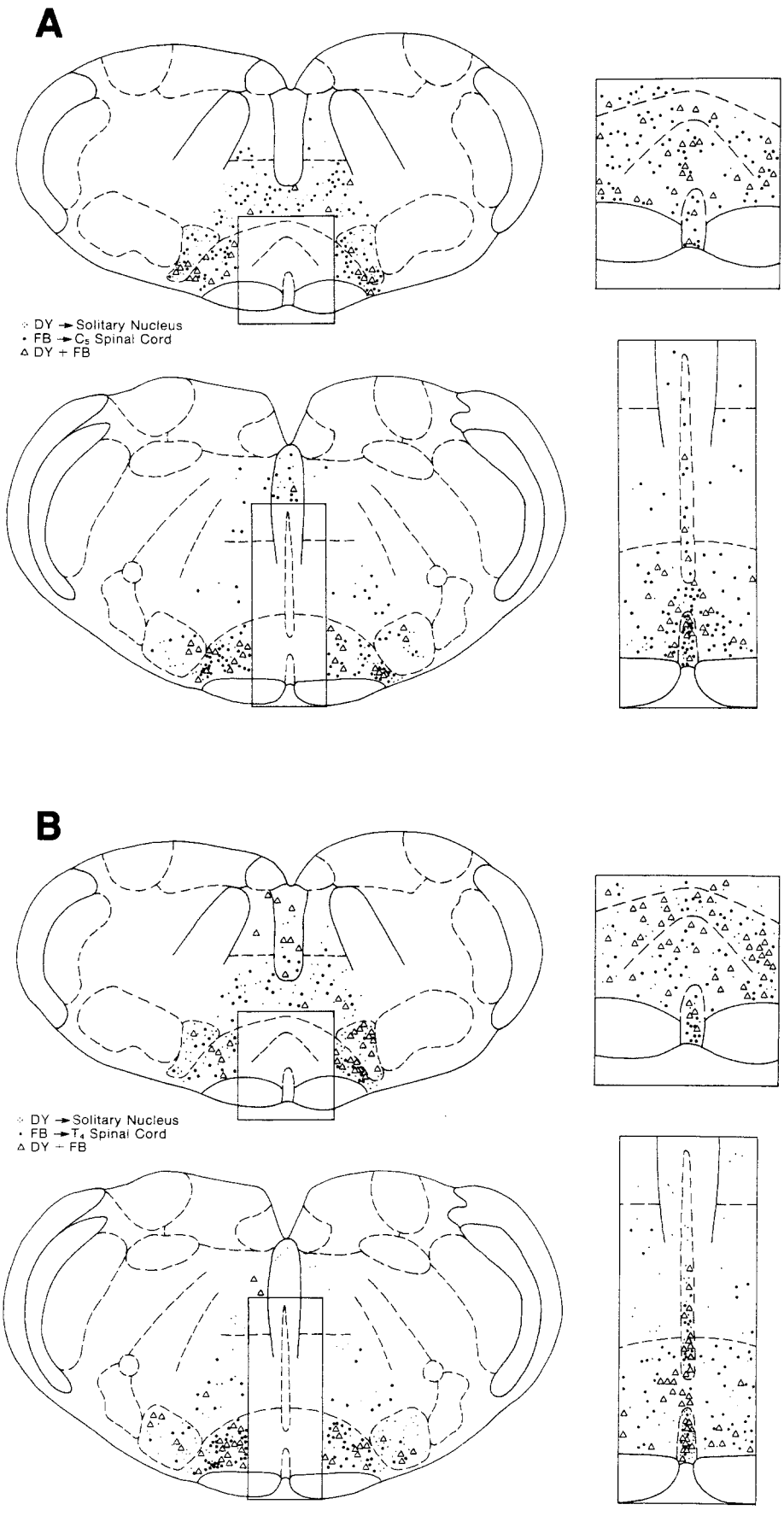

Fig. 3A–C Line drawings depicting representative medial tegmental field labeling after injections of diamidino yellow (*DY*) and fast blue (*FB*). To allow comparison of the distribution of labeled neurons between the three combinations of injections at each pontomedullary level, **A** is from animals with injections of DY into the nucleus of the solitary tract (NST) and FB into the fifth cervical segment, **B** is from animals with injections of DY into the NST and FB into the fourth thoracic segment, and **C** is from animals with injections of DY into the NST and FB into the second lumbar segment. Only labeling within the caudal raphe nuclei and adjacent reticular formation of the medial tegmental field were analyzed and plotted. Within each of the three panels (**A–C**), the *top drawing* is at the level of the nuclei raphe magnus and pallidus, while the *bottom drawing* is at the level of the nuclei raphe obscurus and pallidus. Because of the high density of labeling within the caudal raphe nuclei and adjacent ventromedial reticular formation, these regions have been magnified and shown to the *right* of each brainstem section. Each symbol (*small dot, filled circle, open triangle*) represents a single neuron fluorescently labeled with DY, FB, or both DY and FB, respectively. (*7*, facial nucleus, *DPGi* dorsal paragigantocellular reticular nucleus, *Gi* gigantocellular reticular nucleus, *GiA* gigantocellular reticular nucleus, pars alpha, *IRt* intermediate reticular nucleus, *LPGi* lateral paragigantocellular reticular nucleus, *MVe* medial vestibular nucleus, *mlf* medial longitudinal fasiculus, *PCRtA* parvicellular reticular nucleus, pars alpha, *PrH* prepositus hypoglossi nucleus, *py* pyramidal decussation, *RMg* nucleus raphe magnus, *ROb* nucleus raphe obscurus, *RPa* nucleus raphe pallidus, *Sp5* spinal trigeminal nucleus, *sp5* spinal trigeminal tract, *SpVe* superior vestibular nucleus)

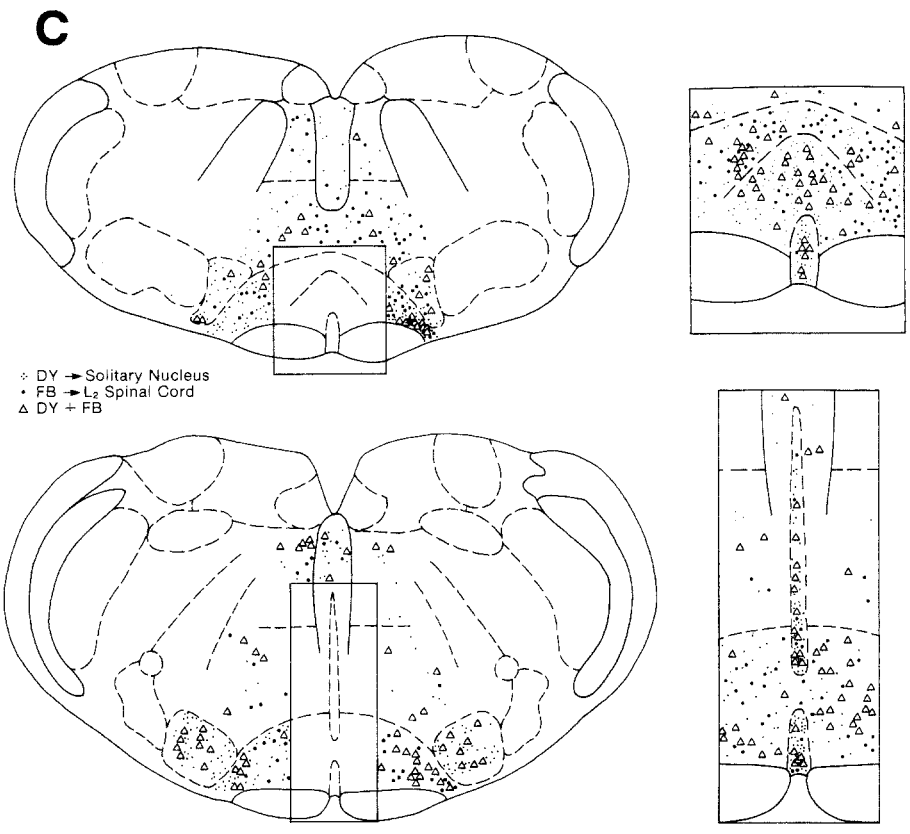
C
DY → Solitary Nucleus
FB → L2 Spinal Cord
DY + FB

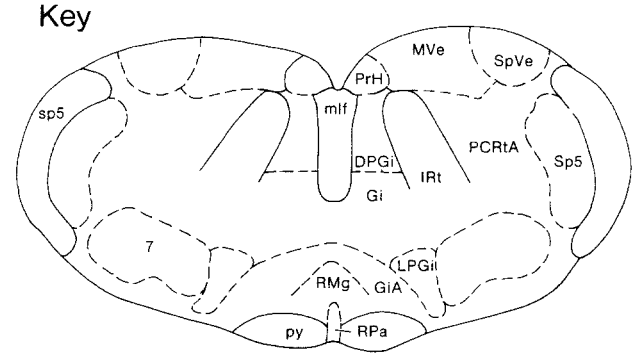
Key
MVe
SpVe
PrH
sp5
mlf
DPGi
PCRtA
Sp5
IRt
Gi
7
LPGi
RMg
GiA
py
RPa

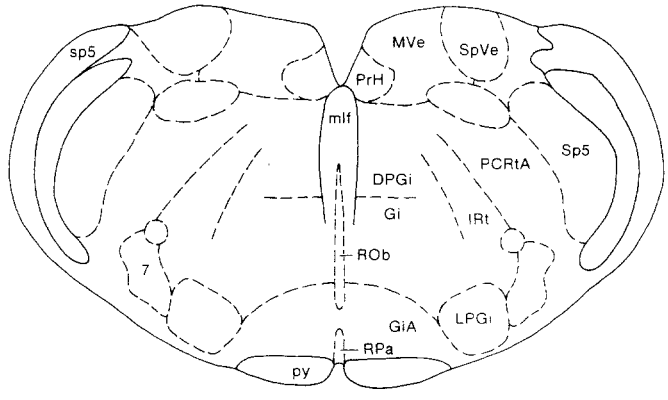
sp5
MVe
SpVe
PrH
mlf
Sp5
PCRtA
DPGi
Gi
IRt
ROb
7
GiA
LPGi
RPa
py

jection site, where only 14% of the neurons projecting to the cervical spinal cord also projected to the NST.

For each of the caudal raphe nuclei, double-labeled neurons were present throughout their rostrocaudal extends. Specifically within the nucleus raphe magnus, there was no apparent difference between the numbers of double-labeled neurons located in the rostral and caudal portions of the nucleus.

Ventromedial reticular formation

Large numbers of double-labeled neurons were observed in both the pars alpha and pars ventralis of the gigantocellular reticular nucleus (Table 2, Fig. 3). In both of these regions, the number of double-labeled neurons ranged from 40 to 60% of the neurons that projected to the NST, except in the gigantocellular reticular nucleus, pars alpha ipsilateral to the injection site following FB instillation into the thoracic spinal cord. In the pars alpha and pars ventralis of the gigantocellular reticular nucleus, greater numbers of neurons were retrogradely labeled by FB injected into the spinal cord at any level than by DY injected into the NST. Therefore, the percentages of raphespinal neurons projecting to the NST (16–48%) were lower than the percentages of neuronal afferents to the NST that projected to the spinal cord.

The lateral paragigantocellular reticular nucleus contained a moderate number of double-labeled neurons compared with the caudal raphe nuclei and the pars alpha and pars ventralis of the gigantocellular reticular nucleus. The largest numbers of neurons retrogradely labeled by DY injected into the NST were observed in the lateral paragigantocellular reticular nucleus bilaterally, where of these neurons only 15–22% ipsilaterally and 11–16% contralaterally also projected to the three different levels of the spinal cord. However, a larger percentage of the neuronal afferents to the spinal cord originating from the lateral paragigantocellular reticular nucleus projected an axon collateral to the NST, particularly those neurons projecting to the lumbar spinal cord, of which over half were double-labeled.

Compared with other regions of the medial tegmental field, the paramedian and the ventral pontine reticular nuclei contained fewer double-labeled neurons that projected to both the NST and the spinal cord. Yet the percentages of neurons projecting to the lumbar spinal cord from these two nuclei that were also retrogradely labeled by DY injected into the NST were surprisingly high. In the ventral pontine reticular nucleus, over 60% of the neurons contralaterally and 53% of the neurons ipsilaterally projecting to the lumbar FB injection site were double-labeled. In the paramedian reticular nucleus, the percentage of neurons projecting to the lumbar spinal cord that were also retrogradely labeled by DY injected into the NST were 34% ipsilateral and 57% contralateral to the injection sites. Lower percentages of neurons projecting to the thoracic or cervical spinal cord from these two nuclei were double-labeled by DY injected into the NST. Likewise, a low to moderate percentage of the neuronal afferents to the NST from these two nuclei also projected an axon collateral to the spinal cord, ranging from 25 to 43% in the paramedian reticular nucleus and 25–46% in the ventral pontine reticular nucleus.

Analysis of control injections

Small-volume injections. To document the presence of double-labeled neurons without use of large tracer volumes, small quantities of DY were injected into the NST in four animals. After injection of 200 nl DY into the NST and 50 nl FB into the cervical spinal cord in three animals, 38±10 double-labeled neurons were observed in the caudal raphe nuclei and adjacent regions of the reticular formation. Similarly, after injection of only 50 nl DY into the NST and 4 µl FB into the cervical spinal cord, 60 double-labeled neurons were noted in the medial tegmental field.

Gracile nucleus injections. No double-labeled neurons were observed anywhere in the medial or lateral tegmental fields, including the caudal raphe nuclei, following injection of 1 µl of DY into the gracile nuclei and 1 µl FB into the cervical spinal cord. After injection of 4 µl FB into the cervical spinal cord, injection of either 1.5 µl or 2 µl of DY into the gracile nucleus produced seven double-labeled neurons in the caudal raphe nuclei and adjacent regions of the reticular formation in each case. In a fourth animal, 4 µl FB was injected into the cervical spinal cord and 1 µl DY was injected into the gracile; however, some DY spread rostrally into a superficial, dorsomedial portion of the NST and resulted in 36 double-labeled neurons present in the medial tegmental field.

Fourth ventricle injections. A series of rats were injected with 4 µl of FB into the cervical spinal cord, and from 1–3 µl DY directly into the fourth ventricle. Injection of 1 µl into the fourth ventricle in two animals produced either 5 or 22 double-labeled neurons in the medial tegmental field. After injection of 2 µl DY into the fourth ventricle in one rat, 29 double-labeled neurons were observed in the caudal raphe nuclei and adjacent regions of the medial tegmental field. In two animals, 3 µl DY injected into the fourth ventricle yielded either 5 or 29 double-labeled neurons in the medial tegmental field.

Discussion

Caudal raphe and adjacent reticular formation neurons send highly collateralized axons to multiple levels of the spinal cord (Hayes and Rustioni 1981; Huisman et al. 1981, 1982; Martin et al. 1981a; Lovick and Robinson 1983). Raphespinal axon collaterals have been demonstrated to the sensory trigeminal nucleus (Lovick and Robinson 1983; Li et al. 1993), periaqueductal gray

(Kwiat and Basbaum, 1990), medial preoptic area (Leanza et al. 1991), and hypoglossal nucleus (Manaker et al. 1992). The current results demonstrate many medial tegmental field neurons that project to the spinal cord, particularly raphespinal neurons, also collateralize to the NST.

Specificity of medial tegmental field neuronal labeling

The descending projections from the ventral part of the medial tegmental field to the spinal cord have been divided into sensory, somatic motor, and autonomic components (Basbaum et al. 1978; Martin et al. 1978; Basbaum and Fields 1979; Holstege et al. 1979; Martin et al. 1979, 1981b, 1982, 1985; Holstege and Kuypers 1982). In the present study, the large volumes of FB injected into the spinal cord, while centered in the somatic motoneuronal regions of cervical and lumbar cord or the autonomic motoneuronal region of thoracic cord, spread throughout the ventral and dorsal grey matter of the spinal cord. As well, spread of the FB occurred into adjacent white matter areas. Therefore, the FB injections are likely to have produced retrograde labeling in all three components of the descending projections to the spinal cord.

Larger numbers of FB-labeled neurons were observed after FB was injected into the cervical than into the thoracic or lumbar spinal cord. This difference in retrogradely labeled FB neuronal somata occurred despite the longer survival intervals utilized for the more caudal spinal injections of FB. Several factors may have contributed to this observation. First, FB uptake into fibers of passage adjacent to the rostral spinal cord injection sites could have produced additional neuronal labeling in the medial tegmental field. Second, intraneuronal dilution of FB within medial tegmental field neurons projecting either longer distances to the lumbar spinal cord or wider axonal arborization patterns could have produced a decrease in the detectability of retrogradely labeled neurons. Third, different numbers of medial tegmental field neurons might project to the different spinal cord segments injected with FB.

Smallest numbers of DY neurons were observed in the medial tegmental field after FB was injected into the cervical than into the thoracic or lumbar spinal cord. This pattern of DY labeling probably reflects the longer survival times employed with more caudal injections of FB, which allowed for greater retrograde transport of DY from the NST injection site to the neuronal somata residing in the medial tegmental field.

The large volume of DY injected into the NST spread into the adjacent structures of the dorsal vagal complex, the area postrema and dorsal vagal motor nucleus, and also into the gracile nucleus. However, control injections of DY directly into the gracile nucleus combined with FB injections into the cervical spinal cord did not produce significant numbers of double-labeled neurons in the medial tegmental field. Furthermore, the caudal raphe nuclei do not project to the gracile nucleus (Basbaum et al. 1978; Holstege and Kuypers 1982). In a similar manner, instillation of large quantities of DY ($\leq$3 µl) directly into the fourth ventricle combined with FB injections into the cervical spinal cord yielded insubstantial numbers of double-labeled neurons in the caudal raphe nuclei and adjacent regions of the reticular formation. Spread of DY from the NST into the fourth ventricle cannot explain our observations, for several reasons. First, the same distributions of double-labeled neurons in the medial tegmental field were noted with the four cases in which less than a full 4 µl of DY was injected into the NST. Second, all of the NST injections of DY were halted when DY appeared at the brainstem surface, and analysis revealed these injection sites to be centered within the NST. Third, even if most of the DY injected into the NST effluxed into the fourth ventricle, the number of double-labeled neurons observed after these injections is many-fold in excess of that observed after injection of DY into the fourth ventricle alone. These observations from our control studies of DY injected into the gracile nucleus or the fourth ventricle combined with FB injected into the cervical spinal cord suggest that the vast majority of neurons retrogradely double-labeled by DY and FB in the current results project to the dorsal vagal complex, as previously demonstrated for medial tegmental field neurons projecting to the dorsal vagal complex (Basbaum et al. 1978; Rogers et al. 1980; Ross et al. 1981; Thor and Helke 1987, 1989; Schaffar et al. 1988; Lynn et al. 1991). The retrograde DY labeling in the present study may reflect medial tegmental field projections specifically to the autonomic motoneurons of the dorsal vagal motor nucleus, to the internuncial neurons in the NST, or to both.

Many double-labeled medial tegmental field neurons that project to the spinal cord and the dorsal vagal complex were identified in the current results, but as discussed above the labeling technique employed precludes identification of the specific terminal fields resulting in retrograde transport of the tracers. Axon collaterals to the spinal cord from double-labeled neurons projecting to the parasympathetic preganglionic motoneurons of the dorsal vagal motor nucleus (Basbaum et al. 1978; Rogers et al. 1980; Ross et al. 1981; Thor and Helke 1987, 1989; Schaffar et al. 1988; Lynn et al. 1991) have several putative targets. Such axon collaterals might project to the sympathetic preganglionic motoneurons of the thoracolumbar intermediolateral column (Holstege et al. 1979; Loewy 1981; Loewy and McKellar 1981; Morrison and Gebber 1984, 1985; Haselton et al. 1988b; Bacon and Smith 1990), the parasympathetic preganglionic motoneurons of the sacral spinal cord (Holstege et al. 1979; Loewy 1981; Loewy and McKellar 1981), or conceivably both. These double-labeled neurons would be predicted to reside within the nuclei raphe obscurus and pallidus and the caudal half of the nucleus raphe magnus, which contain the descending projections to autonomic motoneurons (Basbaum et al. 1978; Martin et al. 1978; Basbaum and Fields 1979; Holstege et al. 1979; Martin

et al. 1979, 1981b, 1982, 1985; Holstege and Kuypers 1982). Similarly, double-labeled neurons that project to the internuncial neurons of the NST (Basbaum et al. 1978; Rogers et al. 1980; Ross et al. 1981; Thor and Helke 1987, 1989; Schaffar et al. 1988; Lynn et al. 1991) are likely to project to sensory interneurons of the dorsal and intermediate grey matter of the spinal cord (Basbaum et al. 1978; Martin et al. 1979; Holstege and Kuypers 1982). These latter double-labeled neurons might be predicted to reside anywhere within the caudal raphe nuclei or adjacent reticular formation, since the rostral nucleus raphe magnus projects to the dorsal horn, the caudal nucleus raphe magnus projects to laminae I and V, and the nuclei raphe pallidus and obscurus project to the spinal intermediate zone (Basbaum et al. 1978; Martin et al. 1978; Basbaum and Fields 1979; Holstege et al. 1979; Martin et al. 1979, 1981b, 1982, 1985; Holstege and Kuypers 1982). In addition, an individual caudal raphe neuron may project to both autonomic motoneurons and internuncial somata and also to somatic motoneurons. The presence of double-labeled somata throughout the rostrocaudal extents of each of the caudal raphe nuclei obviates drawing any inferences about axonal trajectories based upon the previous parcellation of these nuclei into motor, sensory, and autonomic components (Basbaum et al. 1978; Martin et al. 1978; Basbaum and Fields 1979; Holstege et al. 1979; Martin et al. 1979, 1981b, 1982, 1985; Holstege and Kuypers 1982).

Autonomic modulation by medial tegmental field neurons

Neurons in the nuclei raphe pallidus and obscurus and adjacent ventromedial reticular formation widely project to the somatic motoneuron pools within both the spinal cord (Basbaum et al. 1978; Martin et al. 1978; Basbaum and Fields 1979; Holstege et al. 1979; Martin et al. 1979, 1981b, 1982, 1985; Holstege and Kuypers 1982) and the brainstem (Holstege et al. 1977; Borke et al. 1983; Takada et al. 1984; Ugolini et al. 1987; Fort et al. 1989, 1990; Manaker et al. 1992) and manifest axon collaterals to multiple spinal cord levels (Hayes and Rustioni 1981; Huisman et al. 1981, 1982; Martin et al. 1981a; Lovick and Robinson 1983) and to the hypoglossal nucleus (Manaker et al. 1992). Neuronal firing rates within the nuclei raphe pallidus and obscurus vay with behavioral state, with firing rates at nadir during rapid eye movement sleep in association with postural muscle atonia (Heym et al. 1982; Trulson and Trulson 1982; Sakai et al. 1983; Fornal et al. 1985). These data led to the hypothesis that the caudal raphe nuclei globally modulate somatic and autonomic motor activity between different behavioral states (Holstege 1991; Jacobs and Azmitia 1992). The current results document the anatomic substrate for global modulation of the autonomic nervous system.

The nuclei raphe pallidus and obscurus and adjacent ventromedial reticular formation project to the parasympathetic preganglionic motoneurons of the dorsal vagal nucleus (Basbaum et al. 1978; Rogers et al. 1980; Ross et al. 1981; Thor and Helke 1987, 1989; Schaffar et al. 1988; Lynn et al. 1991) and the sacral spinal cord (Holstege et al. 1979; Loewy 1981; Loewy and McKellar 1981), and to the sympathetic preganglionic motoneurons of the thoracolumbar spinal cord (Holstege et al. 1979; Loewy 1981, Loewy and McKellar 1981; Morrison and Gebber 1984, 1985; Haselton et al. 1988b; Bacon and Smith 1990). Electrical (Coote and MacLeod 1974; Neumayr et al. 1974; Cabot et al. 1979; Yen et al. 1983; McCall 1984; Morrison and Gebber 1984, 1985) or chemical (Henry and Calaresu 1974; Minson et al. 1987; Haselton et al. 1988a) stimulation of the caudal raphe nuclei predominantly inhibits sympathetic nerve activity and thereby reduces blood pressure (Coote and Macleod 1974; McCall 1984; Minson et al. 1987), although some sympathoexcitatory effects have been observed (Adair et al. 1977; Futuro-Neto and Coote 1982; Morrison and Gebber 1982). Stimulation of the caudal raphe nuclei also alters parasympathetic tone to the heart (Haselton et al. 1988a) and stomach (McCann et al. 1989; Hornby et al. 1990). These data suggest the caudal raphe nuclei may directly alter the excitability of autonomic motoneurons.

Visceral afferent inputs to the central nervous system may also be modulated by medial tegmental field neurons. The nuclei raphe pallidus and obscurus and adjacent ventromedial reticular formation project to internuncial neurons in the NST (Basbaum et al. 1978; Rogers et al. 1980; Ross et al. 1981; Thor and Helke 1987, 1989; Schaffar et al. 1988; Lynn et al. 1991) and to spinothalamic and other interneurons in the thoracic dorsal horn (Holstege and Kuypers 1982). Spinothalamic neurons receiving sympathetic cardiopulmonary afferent inputs may be inhibited by raphe magnus neurons (Ammons et al. 1984; Chapman et al. 1985; Tattersall et al. 1986). These data support the concept that medial tegmental field neurons can modulate visceral afferent signals to the autonomic nervous system in parallel to the manner in which they modulate nociceptive afferents to the spinal cord (Jacobs and Azmitia 1992). The current results demonstrating that individual medial tegmental field neurons project to both the dorsal vagal complex and the spinal cord suggest that the caudal raphe nuclei may globally modulate both the afferent and the efferent activity of the autonomic nervous system in addition to that of the somatic motoneuron pools.

Modulation of respiratory control by medial tegmental field neurons

Caudal raphe and adjacent medial tegmental field neurons play an important role in respiratory control. The terminal arborizations of caudal raphe axons projecting to the NST (Basbaum et al. 1978; Rogers et al. 1980; Ross et al. 1981; Thor and Helke 1987, 1989; Schaffar et al. 1988; Lynn et al. 1991) are likely to include the respiratory neurons of the ventrolateral subnucleus of the

NST (Saether et al. 1987; Ezure et al. 1988), and caudal raphe neurons also project to the respiratory neuron column of the lateral tegmental field (Connelly et al. 1989; Ellenberger and Feldman 1990; Holtman et al. 1990). Electrical and chemical stimulation of the caudal raphe alters respiratory rate (Polc and Monnier 1970; Sessle et al. 1981; Holtman et al. 1986a, b, 1987; Lalley 1986a, b; Millhorn 1986; Morin et al. 1990). While some studies suggest that the respiratory effects of raphe stimulation are mediated by an intramedullary projection from the raphe nuclei to respiratory neurons which alter phrenic nerve activity (Holtman et al. 1986b; Lalley 1986b), the caudal raphe nuclei may also exert direct effects upon phrenic motoneurons.

The phrenic motor nucleus is composed of somatic motoneurons innervating the diaphragm, but receives a unique group of premotor neural inputs descending from the caudal brainstem rather than propriospinal afferents (Feldman 1986; Holstege 1991). These descending pathways to the phrenic motor nucleus include projections from the caudal raphe nuclei (Holtman et al. 1984). The current results suggest that individual medial tegmental field neurons could simultaneously affect the activities of both NST respiratory neurons and phrenic motoneurons, thereby altering respiration.

Conclusions

Medial tegmental field neurons are known to be highly collateralized, and numerous recent studies have documented diverse projections throughout the neuraxis (Hayes and Rustioni 1981; Huisman et al. 1981, 1982; Martin et al. 1981a; Lovick and Robinson 1983; Leanza et al. 1991; Kwiat and Basbaum 1990; Manaker et al. 1992; Li et al. 1993). However, the full extent of the axonal arborization pattern of an individual caudal raphe neuron remains unknown. The present results suggest that an individual medial tegmental field neuron may globally modulate the activities of autonomic or respiratory pathways by projections to the dorsal vagal complex and the spinal cord. Whether such neurons also project axon collaterals to other regions of the central nervous system concerned with these physiological functions remains to be demonstrated.

Acknowledgements The authors thank Janet Barrow for expert secretarial support and Paola Zucchi for technical assistance. This work has been supported by HL-41169, HL-42236 and an American Lung Association grant. A preliminary report of these results has been published in abstract form (Manaker and Fogarty 1992).

References

Adair JR, Hamilton BL, Scappaticci KA, Helke CJ, Gillis RA (1977) Cardiovascular responses to electrical stimulation of the medullary raphe area of the cat. Brain Res 128:141–145

Altschuler SM, Bao X, Bieger D, Hopkins DA, Miselis RR (1989) Viscerotopic representation of the upper alimentary tract in the rat: sensory ganglia and nuclei of the solitary and spinal trigeminal tracts. J Comp Neurol 283:248–268

Altschuler SM, Ferenci DA, Lynn RB, Miselis RR (1991) Representation of the cecum in the lateral dorsal motor nucleus of the vagus nerve and commissural subnucleus of the nucleus tractus solitarii in rat. J Comp Neurol 304:1–14

Ammons WS, Blair RW, Foreman RD (1984) Raphe magnus inhibition of primate T_1–T_4 spinothalamic cells with cardiopulmonary visceral input. Pain 20:247–260

Andrezik JA, Beitz AJ (1985) Reticular formation, central gray and related tegmental nuclei. In: Paxinos G (ed) Hindbrain and spinal cord. (The rat nervous system, vol 2). Academic, Orlando, pp 1–28

Bacon SJ, Smith AD (1990) Electron microscopic evidence of a monosynaptic pathway between cells in the caudal raphé nuclei and sympathetic preganglionic neurons in the rat spinal cord. Exp Brain Res 79:589–602

Basbaum AJ, Fields HL (1979) The origin of descending pathways in the dorsolateral funiculus of the spinal cord of the cat and rat: further studies on the anatomy of pain modulation. J Comp Neurol 187:513–532

Basbaum AI, Clanton CH, Fields HL (1978) Three bulbospinal pathways from the rostral medulla of the cat: an autoradiographic study of pain modulating systems. J Comp Neurol 178:209–224

Bonham AC, Joad JP (1991) Neurones in commissural nucleus tractus solitarii required for full expression of the pulmonary c-fibre reflex in rat. J Physiol (Lond) 441:95–112

Bonham AC, McCrimmon DR (1990) Neurones in a discrete region of the nucleus tractus solitarius are required for the Breuer-Hering reflex in rat. J Physiol (Lond) 427:261–280

Borke RC, Nau ME, Ringler RL Jr (1983) Brain stem afferents of hypoglossal neurons in the rat. Brain Res 269:47–55

Cabot JB, Wild JM, Cohen DH (1979) Raphe inhibition of sympathetic preganglionic neurons. Science 203:184–186

Carruth MK, Fowler AA, Fairman RP, Mayer DJ, Leichnetz GR (1992) Respiratory failure without pulmonary edema following injection of a glutamate agonist into the ventral medullary raphe of the rat. Brain Res Bull 28:365–378

Chapman CD, Ammons WS, Foreman RD (1985) Raphe magnus inhibition of feline T_1–T_4 spinoreticular tract cell responses to visceral and somatic inputs. J Neurophysiol 53: 773–785

Connelly CA, Ellenberger HH, Feldman JL (1989) Are there serotonergic projections from raphe and retrotrapezoid nuclei to the ventral respiratory group in the rat? Neurosci Lett 105:34–40

Contreras RJ, Beckstead RM, Norgren R (1982) The central projections of the trigeminal, facial, glossopharyngeal and vagus nerves: an autoradiographic study in the rat. J Auton Nerv Syst 6:303–322

Coote JH, MacLeod VH (1974) The influence of bulbospinal monoaminergic pathways on sympathetic nerve activity. J Physiol (Lond) 241:453–475

Ellenberger HH, Feldman JL (1990) Brainstem connections of the rostral ventral respiratory group of the rat. Brain Res 513:35–42

Ezure K, Manabe M, Yamada H (1988) Distribution of medullary respiratory neurons in rat. Brain Res 455:262–270

Feldman JL (1986) Neurophysiology of breathing in mammals. In: Bloom FE (ed) Intrinsic regulatory systems of the brain. (Handbook of physiology, sect 1, The nervous system, vol IV). American Physiological Society, Bethesda, pp 463–524

Finley JCW, Katz DM (1992) The central organization of carotid body afferent projections to the brain stem of the rat. Brain Res 572:108–116

Fornal CA, Auerbach S, Jacobs BL (1985) Activity of serotonin containing neurons in the nucleus raphe pallidus of freely moving cats. Brain Res 251:259–276

Fort P, Sakai K, Luppi PH, Salvert D, Jouvet M (1989) Monoaminergic, peptidergic, and cholinergic afferents to the cat facial nucleus as evidenced by a double immunostaining method with unconjugated cholera toxin as a retrograde tracer. J Comp Neurol 283:285–302

Fort P, Luppi PH, Sakai K, Salvert D, Jouvet M (1990) Nuclei of origin of monoaminergic, peptidergic, and cholinergic affe-

rents to the cat trigeminal motor nucleus: a double-labeling study with cholera toxin as a retrograde tracer. J Comp Neurol 301:262–275

Futuro-Neto HA, Coote JH (1982) Desynchronized sleep-like pattern of sympathetic activity elicited by electrical stimulation of sites in the brainstem. Brain Res 252:269–276

Haselton JR, Winters RW, Liskowsky DR, Haselton CL, McCabe PM, Schneiderman N (1988a) Cardiovascular responses elicited by electrical and chemical stimulation of the rostral medullary raphe of the rabbit. Brain Res 453:167–175

Haselton JR, Winters RW, Liskowsky DR, Haselton CL, McCabe PM, Schneiderman N (1988b) Anatomical and functional connections of neurons of the rostral medullary raphe of the rabbit. Brain Res 453:176–182

Hayes NL, Rustioni A (1981) Descending projections from brainstem and sensorimotor cortex to spinal enlargements in the cat. Exp Brain Res 41:89–107

Henry JL, Calaresu FR (1974) Excitatory and inhibitory inputs from medullary nuclei projecting to spinal cardioacceleratory neurons in the cat. Exp Brain Res 20:485–504

Herbert H, Moga MM, Saper CB (1990) Connections of the parabrachial nucleus with the nucleus of the solitary tract and the medullary reticular formation in the rat. J Comp Neurol 293:540–580

Heym J, Steinfels GF, Jacobs BL (1982) Activity of serotonin-containing neurons in nucleus raphe magnus in freely moving cats. Exp Neurol 88:590–608

Holstege G (1991) Descending motor pathways and the spinal motor system: limbic and non-limbic components. Prog Brain Res 87:307–421

Holstege G, Kuypers HGJM (1977) Fibre connections to the trigeminal, facial and hypoglossal motor nuclei in the cat. I. A lesion-degeneration study. Brain 100:239–264

Holstege G, Kuypers HGJM (1982) The anatomy of brain stem pathways to the spinal cord in cat. A labeled amino acid tracing study. Prog Brain Res 57:145–175

Holstege G, Kuypers HGJM, Dekker JJ (1977) The organization of the bulbar fibre connections to the trigeminal, facial and hypoglossal motor nuclei. II. An autoradiographic tracing in cat. Brain 100:265–286

Holstege G, Kuypers HGJM, Boer RC (1979) Anatomical evidence for direct brain stem projections to the somatic motoneuronal cell groups and autonomic preganglionic cell groups in cat spinal cord. Brain Res 171:329–333

Holtman JR Jr, Norman WP, Gillis RA (1984) Projections from the raphe nuclei to the phrenic motor nucleus in the cat. Neurosci Lett 44:105–111

Holtman JR Jr, Anastasi NC, Norman WP, Dretchen KL (1986a) Effect of electrical and chemical stimulation of the raphe obscurus on phrenic nerve activity in the cat. Brain Res 362:214–220

Holtman JR Jr, Dick TE, Berger AJ (1986b) Involvement of serotonin in the excitation of phrenic motoneurons evoked by stimulation of the raphe obscurus. J Neurosci 6:1185–1193

Holtman JR Jr, Dick TE, Berger AJ (1987) Serotonin-mediated excitation of recurrent laryngeal and phrenic motoneurons evoked by stimulation of the raphe obscurus. Brain Res 417:12–20

Holtman JR Jr, Marion LJ, Speck DF (1990) Origin of serotonin-containing projections to the ventral respiratory group in the rat. Neuroscience 37:541–552

Hornby PJ, Rossiter CD, White RL, Norman WP, Kuhn DH, Gillis RA (1990) Medullary raphe: a new site vor vagally mediated stimulation of gastric motility in cats. Am J Physiol 258:G637–G647

Horst GJ ter, De Boer P, Luiten PGM, Van Willigen JD (1989) Ascending projections from the solitary tract nucleus to the hypothalamus. A *Phaseolus vulgaris* lectin tracing study in the rat. Neuroscience 31:785–797

Huisman AM, Kuypers HGJM, Verburgh CA (1981) Quantitative differences in collateralization of the descending spinal pathways from red nucleus and other brainstem cell groups in rat as demonstrated with the multiple fluorescent retrograde tracer technique. Brain Res 209:271–286

Huisman AM, Kuypers HGJM, Verburgh CA (1982) Differences in collateralization of the descending spinal pathways from red nucleus and other brainstem cell groups in cat and monkey. Prog Brain Res 57:185–217

Jacobs BL, Azmitia EC (1992) Structure and function of the brain serotonin system. Physiol Rev 72:165–229

Kalia M, Sullivan JM (1982) Brainstem projections of sensory and motor components of the vagus nerve in the rat. J Comp Neurol 211:248–264

Kuypers HGJM, Huisman AM (1984) Fluorescent neuronal tracers. Adv Cell Neurobiol 5:307–340

Kwiat GC, Basbaum AI (1990) Organization of tyrosine hydroxylase- and serotonin-immunoreactive brainstem neurons with axon collaterals to the periaqueductal gray and the spinal cord in the rat. Brain Res 528:83–94

Lalley PM (1986a) Responses to phrenic motoneurons of the cat to stimulation of medullary raphe nuclei. J Physiol (Lond) 380:349–371

Lalley PM (1986b) Serotonergic and non-serotonergic responses of phrenic motoneurons to raphe stimulation in the cat. J Physiol (Lond) 380:373–385

Leanza G, Pellitteri R, Russo A, Stanzani S (1991) Neurons in raphe nuclei pontis and magnus have branching axons that project to medial preoptic area and cervical spinal cord. A fluorescent retrograde double labeling study in the rat. Neurosci Lett 123:195–199

Leslie RA, Gwyn DG, Hopkins DA (1982) The central distribution of the cervical vagus nerve and gastric afferent and efferent projections in the rat. Brain Res Bull 8:37–53

Li Y-Q, Takada M, Shinonaga Y, Mizuno N (1993) Collateral projections of single neurons in the nucleus raphe magnus to both the sensory trigeminal nuclei and spinal cord in the rat. Brain Res 602:331–335

Loewy AD (1981) Raphe pallidus and raphe obscurus projections to the intermediolateral cell column in the rat. Brain Res 222:129–133

Loewy AD, Burton H (1978) Nuclei of the solitary tract: efferent connections to the lower brainstem and spinal cord of the cat. J Comp Neurol 181:421–450

Loewy AD, McKellar S (1981) Serotonergic projections from the ventral medulla to the intermediolateral cell column in the rat. Brain Res 211:146–152

Lovick TA, Robinson JP (1983) Bulbar raphe neurones with projections to the trigeminal nucleus and the lumbar cord in the rat: a fluorescence double-labelling study. Exp Brain Res 50:299–308

Lynn RB, Kreider MS, Miselis RR(1991) Thyrotropin-releasing hormone-immunoreactive projections to the dorsal motor nucleus and the nucleus of the solitary tract of the rat. J Comp Neurol 311:271–288

Manaker S, Tischler LJ, Morrison AR (1992) Raphespinal and reticulospinal axon collaterals to the hypoglossal nucleus in the rat. J Comp Neurol 332:68–78

Manaker S, Fogarty PF (1992) Raphespinal neurons project axon collaterals to the nucleus of the solitary tract. Am Rev Resp Dis 145:A408

Martin GF, Humbertson AO Jr, Laxson LC, Panneton WM (1979) Evidence for direct bulbospinal projections to laminae IX, X and the intermediolateral cell column. Studies using axonal transport techniques in the North American opossum. Brain Res 170:165–171

Martin GF, Cabana T, Humbertson AO Jr (1981a) Evidence for collateral innervation of the cervical and lumbar enlargements of the spinal cord by single reticular and raphe neurons. Studies using fluorescent markers in double-labeling experiments on the North American opossum. Neurosci Lett 24:1–6

Martin GF, Cabana T, Humbertson AO Jr, Laxson LC, Panneton WM (1981b) Spinal projections from the medullary reticular formation of the North American opposum: evidence for connectional heterogeneity. J Comp Neurol 196:663–682

Martin GF, Cabana T, Ditirro FJ, Ho RH, Humbertson AO Jr (1982) Raphespinal projections in the North American opposum: evidence for connectional heterogeneity. J Comp Neurol 208:67–84

Martin GF, Vertes RP, Waltzer R (1985) Spinal projections of the gigantocellular reticular formation in the rat. Evidence for projections from different areas to laminae I and II and lamina IX. Exp Brain Res 58:154–162

Martin RF, Jordan LM, Willis WD (1978) Differential projections of cat medullary raphe neurons demonstrated by retrograde labelling following spinal cord lesions. J Comp Neurol 182:77–88

McCall RB (1984) Evidence for a serotonergically mediated sympathoexcitatory response to stimulation of medullary raphe nuclei. Brain Res 311:131–139

McCann MJ, Hermann GE, Rogers RC (1989) Nucleus raphe obscurus (nRO) influences vagal control of gastric motility in rats. Brain Res 486:181–184

Millhorn DE (1986) Stimulation of the raphe (obscurus) nucleus causes long-term potentiation of phrenic nerve activity in cat. J Physiol (Lond) 381:169–179

Minson JB, Chalmers JP, Caon AC, Renaud B (1987) Separate areas of rat medulla oblongata with populations of serotonin- and adrenaline-containing neurons alter blood pressure after L-glutamate stimulation. J Auton Nerv Syst 19:39–50

Morin D, Hennequin S, Monteau R, Hilaire G (1990) Depressant effect of raphe stimulation on inspiratory activity of the hypoglossal nerve: in vitro study in the newborn rat. Neurosci Lett 116:299–303

Morrison SF, Gebber GL (1982) Classification of raphe neurons with cardiac-related activity. Am J Physiol 243:R49–R59

Morrison SF, Gebber GL (1984) Raphe neurons with sympathetic-related activity: baroreceptor responses and spinal connections. Am J Physiol 84:R338–R348

Morrison SF, Gebber GL (1985) Axonal branching patterns and funicular trajectories of raphespinal sympathoinhibitory neurons. J Neurophysiol 53:759–772

Neumayr RJ, Hare BD, Franz DN (1974) Evidence for bulbospinal control of sympathetic preganglionic neurons by monoaminergic pathways. Life Sci 14:793–806

Newman DB (1985a) Distinguishing rat brainstem reticulospinal nuclei by their neuronal morphology. I. Medullary nuclei. J Hirnforsch 26:187–226

Newman DB (1985b) Distinguishing rat brainstem reticulospinal nuclei by their neuronal morphology. II. Pontine and mesencephalic nuclei. J Hirnforsch 26:385–448

Norgren R (1978) Projections from the nucleus of the solitary tract in the rat. Neuroscience 3:207–218

Paxinos G, Watson C (1986) The rat brain in stereotaxic coordinates, 2nd edn. Academic, San Diego

Polc P, Monnier M (1970) An activating mechanism in the pontobulbar raphe system of the rabbit. Brain Res 22:47–61

Ricardo JA, Koh ET (1978) Anatomical evidence of direct projections from the nucleus of the solitary tract to the hypothalamus, amygdala, and other forebrain structures in the rat. Brain Res 153:1–26

Rogers RC, Kita H, Butcher LL, Novin D (1980) Afferent projections to the dorsal motor nucleus of the vagus. Brain Res Bull 5:365–373

Ross CA, Ruggiero DA, Reis DJ (1981) Afferent projections to cardiovascular portions of the nucleus of the tractus solitarius in the rat. Brain Res 223:402–408

Ross CA, Ruggiero DA, Reis DJ (1985) Projections from the nucleus tractus solitarii to the rostral ventrolateral medulla. J Comp Neurol 242:511–534

Saether K, Hilaire G, Monteau R (1987) Dorsal and ventral respiratory groups of neurons in the medulla of the rat. Brain Res 419:87–96

Sakai K, Vanni-Mercier G, Jouvet M (1983) Evidence for the presence of PS-OFF neurons in the ventromedial medulla oblongata of freely moving cats. Exp Brain Res 49:311–314

Saper CB, Loewy AD (1980) Efferent connections of the parabrachial nucleus in the rat. Brain Res 197:291–311

Saper CB, Loewy AD, Swanson LW, Cowan WM (1976) Direct hypothalamo-autonomic connections. Brain Res 117:305–312

Sawchenko PE (1983) Central connections of the sensory and motor nuclei of the vagus nerve. J Auton Nerv Syst 9:13–26

Sawchenko PE, Swanson LW (1982) Immunohistochemical identification of neurons in the paraventricular nucleus of the hypothalamus that project to the medulla or to the spinal cord in the rat. J Comp Neurol 205:260–272

Schaffar N, Kessler JP, Bosler O, Jean A (1988) Central serotonergic projections to the nucleus tractus solitarii: evidence from a double labeling study in the rat. Neuroscience 26:951–958

Sessle BJ, Ball GJ, Lucier GE (1981) Suppressive influences from periaqueductal gray and nucleus raphe magnus on respiration and related reflex activities and on solitary tract neurons, and effect of naloxone. Brain Res 216:145–161

Shapiro RE, Miselis RR (1985) The central organization of the vagus nerve innervating the stomach of the rat. J Comp Neurol 238:473–488

Smith JC, Morrison DE, Ellenberger HH, Otto MR, Feldman JL (1989) Brainstem projections to the major respiratory neuron populations in the medulla of the cat. J Comp Neurol 281:69–96

Spyer KM (1982) Central nervous integration of cardiovascular control. J Exp Biol 100:109–128

Takada M, Itoh K, Yasui Y, Mitani A, Nomura S, Mizuno N (1984) Distribution of premotor neurons for the hypoglossal nucleus in the cat. Neurosci Lett 52:141–146

Tattersall JEH, Cervero F, Lumb BM (1986) Viscerosomatic neurons in the lower thoracic spinal cord of the cat: excitations and inhibitions evoked by splanchnic and somatic nerve volleys and by stimulation of brain stem nuclei. J Neurophysiol 56:1411–1423

Thor KB, Helke CJ (1987) Serotonin- and substance P-containing projections to the nucleus tractus solitarii of the rat. J Comp Neurol 265:275–293

Thor KB, Helke CJ (1989) Serotonin and substance P colocalization in medullary projections to the nucleus tractus solitarius: dual-colour immunohistochemistry combined with retrograde tracing. J Chem Neuroanat 2:139–148

Trulson ME, Trulson VM (1982) Activity of nucleus raphe pallidus neurons across the sleep-waking cycle in freely moving cats. Brain Res 237:232–237

Ugolini G, Kuypers HGJM, Simmons A (1987) Retrograde transneuronal transfer of Herpes simplex virus type I (HSV 1) from motoneurons. Brain Res 422:242–256

Van der Kooy D, Koda LY, McGinty JF, Gerfen CR, Bloom FE (1984) The organization of projections from the cortex, amygdala, and hypothalamus to the nucleus of the solitary tract in rat. J Comp Neurol 224:1–24

Yamada H, Ezure K, Manabe M (1988) Efferent projections of inspiratory neurons of the ventral respiratory group. A dual labeling study in the rat. Brain Res 455:283–294

Yen C-T, Blum PS, Spath JA Jr (1983) Control of cardiovascular function by electrical stimulation within the medullary raphe region of the cat. Exp Neurol 79:666–679